

## PDF hosted at the Radboud Repository of the Radboud University Nijmegen

The following full text is a publisher's version.

For additional information about this publication click this link.

<http://hdl.handle.net/2066/17394>

Please be advised that this information was generated on 2022-08-24 and may be subject to change.

# Induction of male sterility in plants by a chimaeric ribonuclease gene

Celestina Mariani\*, Marc De Beuckeleer\*, Jessie Truettner†, Jan Leemans\* & Robert B. Goldberg†‡

\* Plant Genetic Systems NV, J. Plateaustraat 22, B-9000 Gent, Belgium

† Department of Biology, University of California, Los Angeles, California 90024-1606, USA

Chimaeric ribonuclease genes that are expressed in the anthers of transformed tobacco and oilseed rape plants were constructed. Chimaeric ribonuclease gene expression within the anther selectively destroys the tapetal cell layer that surrounds the pollen sac, prevents pollen formation, and leads to male sterility. These nuclear male sterility genes should facilitate the production of hybrid seed in various crop plants.

MALE reproductive processes in flowering plants occur in the anther<sup>1</sup>. This organ is composed of several tissues and cell types, contains several thousand anther-specific messenger RNAs<sup>2,3</sup>, and is responsible for producing pollen grains that contain the sperm cells. A specialized anther tissue, the tapetum, plays an important part in pollen formation<sup>1,4-6</sup>. The tapetum surrounds the pollen sac early in anther development, degenerates during the later stages of development, and is not present as an organized tissue in the mature anther<sup>1</sup>. The tapetum produces a number of proteins and other substances that either aid in pollen development or become components of the pollen outer wall<sup>1,4,6</sup>.

Cytoplasmic and nuclear mutations have been identified that prevent normal pollen development and result in male sterility<sup>7</sup>. Many male sterility mutations interfere with tapetal cell differentiation and/or function, indicating that this tissue is essential for the production of functional pollen grains<sup>7</sup>. Male sterility mutations have proved useful for producing hybrids beneficial in increasing crop productivity<sup>7</sup>. Hybrid production, however, has been limited to those plants in which male sterile lines that can be restored to fertility have been identified, and/or those in which mechanical removal of anthers from flowers is both possible and practical<sup>7</sup>. The ability to produce hybrid plants in various crops would be greatly facilitated by the availability of a dominant male sterility gene that could be introduced into plant cells by genetic engineering.

Here we report that the 5' region of a tobacco tapetum-specific gene<sup>8,9</sup> can activate the expression of a  $\beta$ -glucuronidase (*GUS*) marker gene and two different ribonuclease (*RNase*) genes within the tapetal cells of transgenic tobacco and oilseed rape plants. Expression of the chimaeric *RNase* genes selectively destroys the tapetum during anther development, prevents pollen formation, and leads to the production of male sterile plants.

## Tobacco gene expression in anther tapetum

We previously described the identification of two tobacco anther complementary DNA clones, designated as *TA29* and *TA13*<sup>8</sup>. These cDNA clones are 85% similar at the nucleotide level (J. Seurinck, C.M. and R.B.G., unpublished data), and are both complementary to 1.1- and 1.2-kilobase (kb) anther mRNAs that are undetectable in other floral and vegetative organ systems (Fig. 1). *In situ* hybridization studies with anther sections

showed that the *TA29* and *TA13* mRNAs are both localized within tapetal cells<sup>8</sup>.

DNA gel blot studies indicated that there are less than five *TA29*- and *TA13*-like genes in the tobacco genome, and that related genes exist in many other plants, such as tomato, oilseed rape, lettuce and alfalfa (data not shown). We isolated a clone containing the *TA29* gene by screening a tobacco genome library with the *TA29* cDNA<sup>9</sup>. DNA sequencing studies showed that the *TA29* gene does not contain introns, and that it encodes a glycine-rich (20%) protein of relative molecular mass 33,000 ( $M_r$  33K) with potential glycosylation sites<sup>9</sup>. Together, our results indicate that the *TA29* gene is expressed specifically in anther tapetal cells, is present in distantly related plant species, and encodes a protein that has properties similar to some plant cell wall proteins<sup>10-12</sup>.

## Control of tapetal-specific expression

Transcription studies with RNAs synthesized in isolated anther and leaf nuclei demonstrated that the *TA29* gene is regulated primarily at the transcriptional level (A. Koltunow and R.B.G., unpublished results). To demonstrate that 5' sequences control *TA29* gene developmental specificity, we fused the *Escherichia coli GUS* gene<sup>13</sup> with a 1.5-kb *TA29* gene upstream fragment (nucleotides -1,477 to +51; ref. 9) containing the start codon,

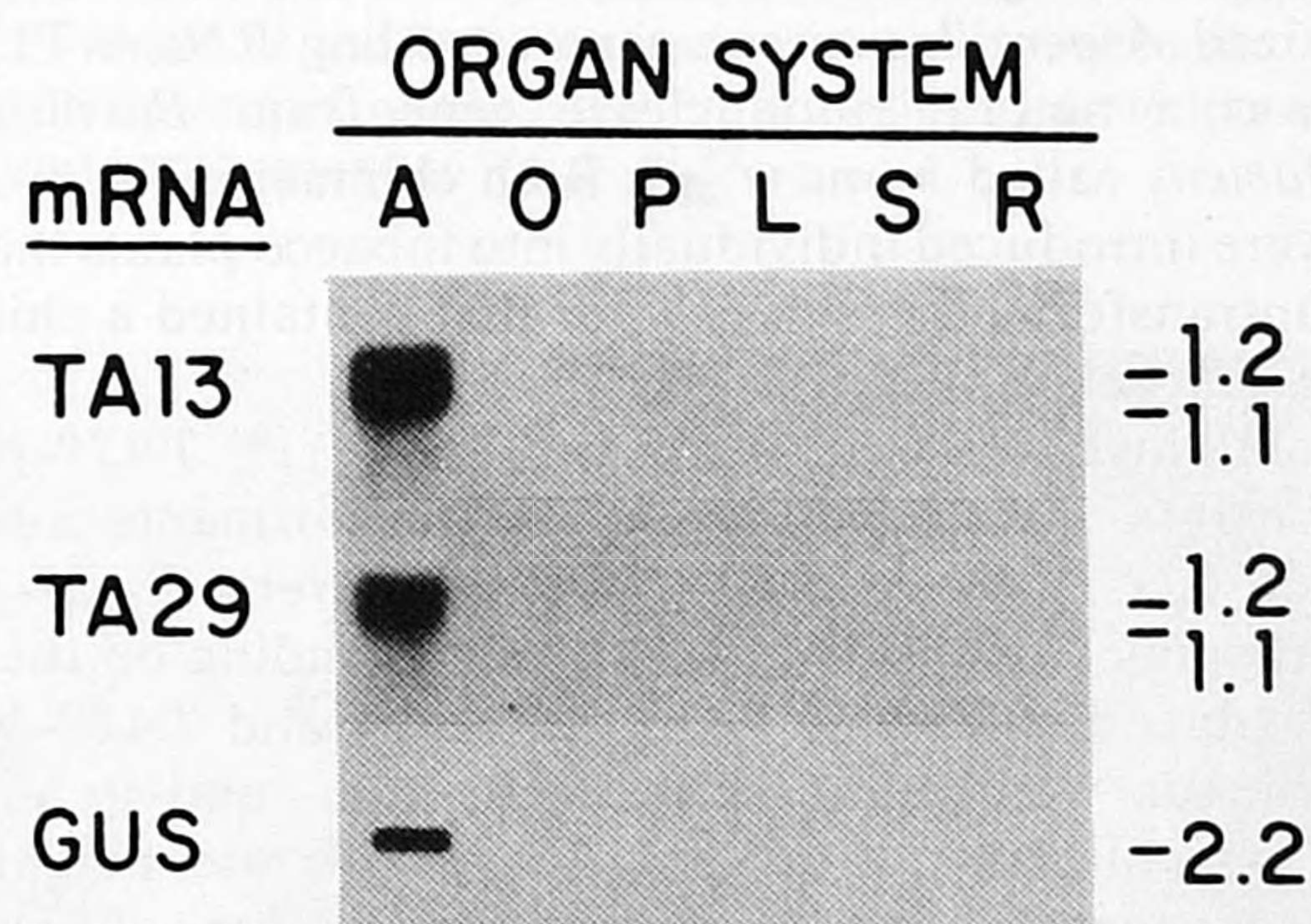


FIG. 1 Organ-specific *TA29* and *TA29-GUS* gene expression patterns. Tobacco anther (A), ovary (O), petal (P), leaf (L), stem (S), and root (R) RNA gel blots were hybridized with either labelled cDNA plasmids (*TA13* and *TA29*) or with a labelled anti-mRNA probe (*GUS*). Tobacco plants from which vegetative organ systems were collected, as well as flower developmental stages, were described previously<sup>2,3,8,21</sup>. Polysomal poly(A)<sup>+</sup> mRNAs (1  $\mu$ g) from untransformed plants were used for the *TA13* and *TA29* gel blots. Total RNAs (10  $\mu$ g) from a plant transformed with the chimaeric *TA29-GUS* gene were used for the *GUS* gel blot. Autoradiograms were exposed for ~2 h. DNA size markers (kb) to the right.

METHODS. RNAs were isolated as described<sup>2,3,21</sup>. RNA gel blot experiments and labelling of DNA and RNA probes were as described<sup>21,22</sup>. The *TA29-GUS* gene was introduced into a cointegration vector that contains the bialaphos resistance gene (*bar*) as a selectable marker<sup>18,19</sup>. The *TA29-GUS* gene was transferred to tobacco (*Nicotiana tabacum* cv. 'SR-1') using standard *Agrobacterium* transformation procedures<sup>18,19,23,24</sup>.

‡ To whom correspondence should be addressed.

and then transformed tobacco plants with the chimaeric *TA29-GUS* gene. We generated 13 independent transformants that contained from one to three unrearranged copies of the *TA29-GUS* gene (data not shown). Although the levels varied, the anthers of each transformant contained both *GUS* mRNA and enzyme activity, suggesting that the chimaeric *TA29-GUS* gene was regulated correctly (data not shown).

We hybridized a *GUS* gene probe with different RNAs from one transformant, designated as N102-2, to determine the *TA29-GUS* gene organ specificity. This plant expressed the *TA29-GUS* gene at a level that was about average for all our transformants. *GUS* mRNA was observed only in the anther, and was undetectable in other organ systems (Fig. 1). Experiments with anthers at different developmental stages showed that both *GUS* mRNA and enzyme activity accumulated and decayed in parallel with tapetal cell appearance and disintegration, and were coordinated with changes in endogenous *TA29* mRNA levels (data not shown).

We hybridized *TA29* and *GUS* anti-mRNA probes with adjacent N102-2 anther sections *in situ* to compare the cell-specific expression pattern of the *TA29-GUS* gene with that of the endogenous *TA29* gene. Figure 2*a* and *b* shows bright field photographs of anther sections at two developmental stages<sup>8</sup>. Intense hybridization grains were produced by the *GUS* anti-mRNA probe exclusively within the tapetum at stage 2 (Fig. 2*g*). By contrast, no *GUS* hybridization grains above background were observed at stage 8 when the tapetum had degenerated (Fig. 2*h*). These hybridization patterns were identical to those produced with the *TA29* anti-mRNA probe (Fig. 2*d, e*). *GUS* enzyme activity was also detected within the tapetum at stage 2 (Fig. 2*i*), and was not detectable in other anther tissues. Together, these data show that the chimaeric *TA29-GUS* gene is regulated exactly like the endogenous *TA29* gene, and that the 1.5-kb *TA29* gene 5' fragment contains all the information required to programme the tapetal-specific expression pattern.

### ***TA29-RNase* gene causes male sterility**

We fused the 1.5-kb *TA29* gene regulatory fragment with two different ribonuclease genes to selectively destroy the tapetal cell lineage during anther development. One was a chemically synthesized *Aspergillus oryzae* gene encoding RNase-T1<sup>14</sup>. The other was a natural ribonuclease gene from *Bacillus amyloliquefaciens* called *barnase*<sup>15,16</sup>. Both chimaeric *TA29-RNase* genes were introduced individually into tobacco plants that were either untransformed previously, or that contained a chimaeric *TA29-GUS* gene (N102-2).

We obtained 20 *TA29-RNase T1* and 115 *TA29-barnase* transformants. Sixty per cent of these transformants contained a single *TA29-RNase* gene. The rest had several *TA29-RNase* inserts ranging from two to six copies, depending on the transformant (data not shown). *TA29-RNase T1* and *TA29-barnase* transformants were identical to each other, and to untransformed control plants, with respect to growth rate, height, morphology of vegetative and floral organ systems, time of flowering, and flower coloration pattern. However, 10% of *TA29-RNase T1* transformants (2/20), and 92% of *TA29-barnase* transformants (106/115) failed to shed pollen (Fig. 3). In contrast to mature untransformed anthers (Fig. 3*a*), anthers on flowers of these plants were shrivelled, greyish-brown in colour, and devoid of pollen grains (Fig. 3*b*).

The pollenless *TA29-RNase* plants failed to produce fruit capsules and seeds; flowers simply senesced and fell off. By contrast, when these plants were cross-pollinated with pollen from untransformed anthers (Fig. 3*a*) fruit capsules developed and normal seed set was obtained. These results indicated that the pollenless *TA29-RNase* plants were male sterile, that their pistils were able to recognize and transmit pollen normally, and that female fertility was unaffected. Progeny from cross-pollinated plants with single-copy *TA29-RNase* inserts segregated 1:1 for male sterility and male fertility, and these phenotypes

correlated directly with the presence or absence of a chimaeric *TA29-RNase* gene (data not shown). Together, these data indicate that the presence of either a chimaeric *TA29-RNase T1* gene or a *TA29-barnase* gene leads to the production of male sterile tobacco plants.

We analysed the male sterile anthers of *TA29-RNase T1* plants for the presence of both *RNase T1* and *TA29* mRNAs. In addition, the anthers of male sterile N102-2 plants (Fig. 2) that contained both the *TA29-RNase T1* and *TA29-GUS* genes were analysed for *GUS* enzyme activity. Hybridization of a *TA29* anti-mRNA probe with stage 2 anther sections *in situ* revealed only residual amounts of endogenous *TA29* mRNA (Fig. 2*f*). This result contrasted with the intense tapetal-specific signals obtained with anthers containing the *TA29-GUS* gene (Fig. 2*d, g*). Hybridization of adjacent sections with a *RNase T1* anti-mRNA probe failed to produce hybridization grains above background (data not shown). RNA dot blot experiments showed that *RNase T1* mRNA was present in male sterile anthers, but only at a period before the time of maximum *TA29* mRNA accumulation in untransformed plants (stage 1 versus stage 3). In addition, the *RNase T1* mRNA level was at least 100-fold lower than that of either *TA29* mRNA or *GUS* mRNA in anthers containing only the *TA29-GUS* gene (data not shown). In contrast to the high tapetal-specific *GUS* enzyme activity in N102-2 anthers (Fig. 2*i*), *GUS* enzyme activity was undetectable in male sterile anthers that contained both *TA29-RNase* and *TA29-GUS* genes (data not shown). Together these data show that the male sterility phenotype is associated with a dramatic decrease in tapetal-specific mRNA levels, and that this decrease is correlated with the presence of a chimaeric *TA29-RNase* gene.

### **Selective destruction of the tapetum**

We compared anther development in male sterile tobacco plants containing either the *TA29-RNase T1* or *TA29-barnase* genes to that of untransformed control plants. No differences were observed from stage 1 (0.8 cm flower bud) to stage 12 (open flower) with respect to timing, colour, changes in size and weight, external morphology and filament length. In addition, the male sterile anthers dehisced correctly at flower opening. The single difference between male sterile and male fertile anthers was the apparent absence of pollen grains (Fig. 3*a, b*).

We prepared transverse tobacco anther sections at each stage of development to compare the tissue differentiation patterns of male sterile and male fertile anthers. Figures 2 and 4 show bright field photographs of stage 2 anthers from male fertile plants (Figs 2*a* and 4*a*), and male sterile plants containing a *TA29-RNase* gene (Figs 2*c* and 4*b*). Male fertile anthers contained a prominent tapetum (T) surrounding a well-formed pollen sac (PS) that was packed with developing pollen grains (Figs 2*a* and 4*a*). By contrast, male sterile anthers lacked a detectable tapetum, and had a collapsed pollen sac without visible microspores or pollen grains (Figs 2*c* and 4*b*). All other tissues and cell types were identical in male sterile and male fertile anthers (Fig. 4). Together these data indicate that the presence of a chimaeric *TA29-RNase* gene selectively destroys the tapetum during anther development.

### **Male sterile anthers do not produce pollen**

No pollen grains were observed in any of the 106 male sterile tobacco plants containing a chimaeric *TA29-barnase* gene. By contrast, we obtained a small number of pollen-like structures from dehiscent male sterile tobacco anthers containing the *TA29-RNase T1* gene. These pollen-like structures either failed to germinate or produced abnormal pollen tubes, could not successfully pollinate the pistils of either male sterile or male fertile plants, and were 100-fold less prevalent than pollen grains produced by male fertile anthers (data not shown). We visualized these pollen-like structures in the scanning electron microscope. The abnormal pollen (MS) from male sterile anthers is ~50-fold

smaller in size than normal tobacco pollen grains (WT) (Fig. 5a). Higher magnification of these abnormal pollen grains shows that they do not have a normal exine, lack a groove or sulcus, and are irregular in shape (Fig. 5b). Together, these results indicate that the selective destruction of the tapetum by the expression of the chimaeric *TA29-RNase T1* gene or

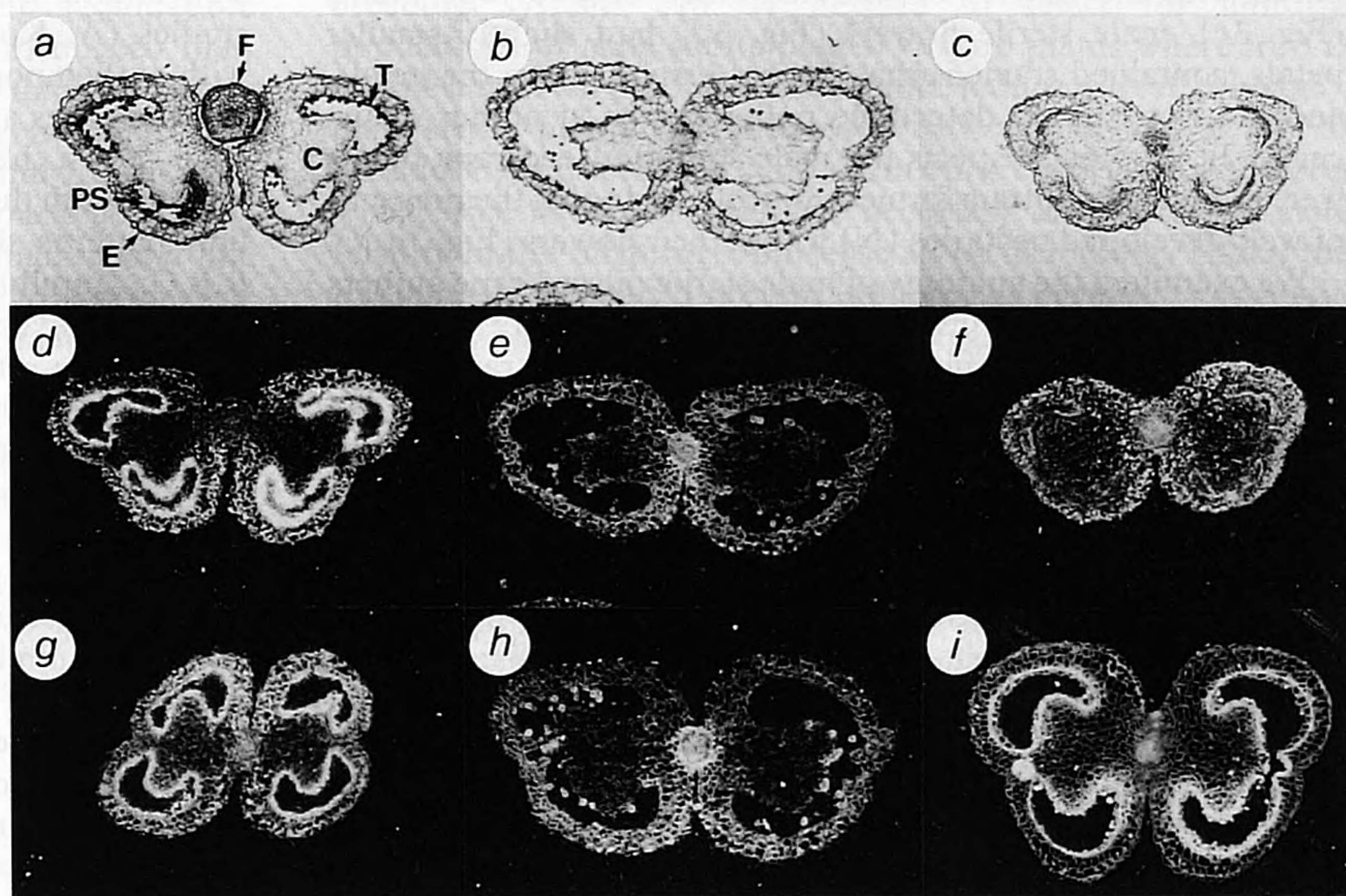
the *TA29-barnase* gene blocks tobacco pollen grain development.

### *TA29-RNase* expression in other plants

We transformed oilseed rape plants (*Brassica napus* cv. 'Drakkar') with the chimaeric *TA29-RNase T1* and *TA29-barnase*

FIG. 2 Localization of *TA29* and *TA29-GUS* gene expression patterns in tobacco anthers. *a* and *b*, Bright field photographs of anthers containing the *TA29-GUS* gene at stage 2 (*a*) and stage 8 (*b*) of flower development<sup>8</sup>. C, E, F, PS and T refer to connective, epidermis, filament, pollen sac and tapetum, respectively. *c*, Bright field photograph of an anther containing the *TA29-RNase T1* gene at flower development stage 2 (ref. 8). *d* and *e*, *In situ* hybridization of a *TA29* anti-mRNA probe with anthers containing the *TA29-GUS* gene at flower development stage 2 (*d*) and stage 8 (*e*). Photographs taken by dark field microscopy. White grains represent regions containing RNA-RNA hybrids. Hybridization grains produced with stage 8 anthers were not detectably greater than those produced with a *TA29* mRNA control probe (data not shown). *f*, *In situ* hybridization of a *TA29* anti-mRNA probe with anthers containing a *TA29-RNase* gene at flower development stage 2 (ref. 8). Anthers from a *TA29-RNase T1* transformant were used for this experiment. Photograph taken by dark field microscopy. White regions along the anther wall represent dark-field light scattering through the stained anther section. Identical results were obtained with a *TA29* mRNA control probe (data not shown). White grains outlining the residual tapetum represent RNA-RNA hybrids, and were only 10-fold greater in density than background grains in adjacent connective tissue. *g* and *h*, *In situ* hybridization of a *GUS* anti-mRNA probe with anthers containing the *TA29-GUS* gene at flower development stage 2 (*g*) and stage 8 (*h*). Sections were taken from the same fixed anthers used for the experiments shown in Fig. 2*d*, *e*. Photographs taken with dark field microscopy. White grains, regions of RNA-RNA hybridization. Grains produced with stage 8 anthers (*h*) represent background hybridization, and were not significantly greater than those produced with a *GUS* mRNA control probe (data not shown). *i*, Localization of *GUS* enzyme activity in stage 2 anthers containing the *TA29-GUS* gene. Pink areas, regions with enzyme activity. Photograph taken with dark field microscopy.

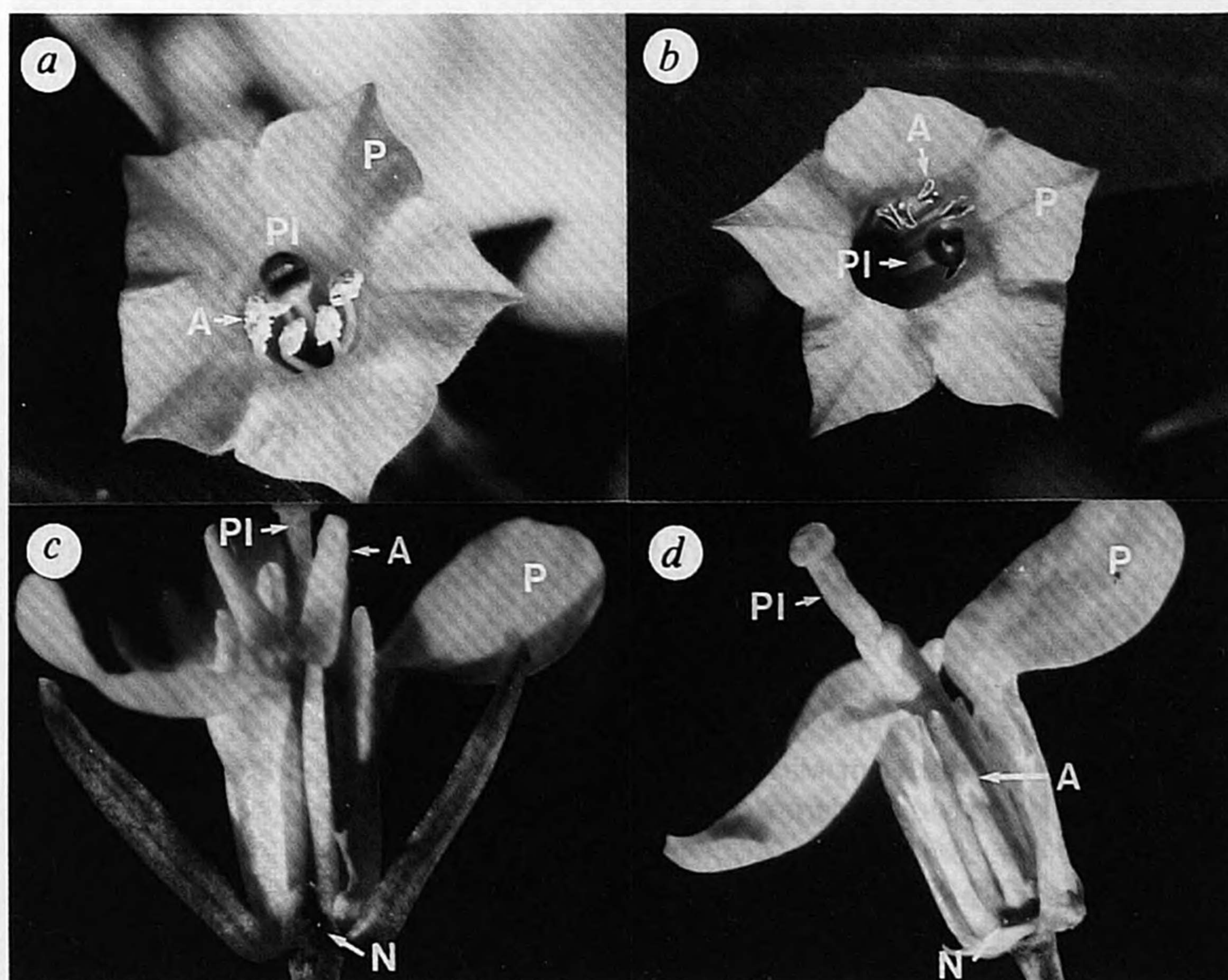
METHODS. Anthers at the relevant stage were collected, and their ends



sliced off with a razor blade to facilitate fixative penetration. Paraffin-embedded anther sections were hybridized *in situ* with single-stranded <sup>35</sup>S-labelled-anti-mRNA and <sup>35</sup>S-labelled mRNA (control) probes exactly as described<sup>21</sup>. Autoradiography and photography techniques used for the hybridized sections were published previously<sup>21,25</sup>. All photographs were taken with the same magnification. *GUS* enzyme activity was localized by incubating unfixed, tipless anthers in 50 mM phosphate buffer, pH 7 containing 1 mM X-Glu (ref. 13) for several hours at 37 °C. After a visible histochemical reaction occurred, the anthers were fixed in glutaraldehyde<sup>21</sup>, embedded in LR-white resin (Polysciences), and sectioned with a glass knife. The *TA29-RNase T1* and *TA29-barnase* genes were recloned into cointegration and binary vectors, respectively<sup>19,26</sup>, and introduced into tobacco plants as outlined in the legend to Fig. 1.

FIG. 3 Male sterile tobacco and oilseed rape flowers. *a* and *b*, Tobacco flowers from untransformed plants (*a*), and plants transformed with *TA29-RNase* gene (*b*). A, P and PI, anther, petal and pistil, respectively. *c* and *d*, Oilseed rape flowers from untransformed plants (*c*), and plants transformed with a *TA29-RNase* gene (*d*). A, P, PI and N, anther, petal, pistil and nectar, respectively.

METHODS. The *TA29-RNase T1* and *TA29-barnase* genes were transferred to a binary vector<sup>26</sup> containing the *bar* gene<sup>18</sup>. Oilseed rape hypocotyls (*Brassica napus* cv. 'Drakkar') were transformed with *Agrobacterium* according to the procedure of De Block *et al.*<sup>27</sup> using bialaphos resistance (*bar*) as a selectable marker.



genes to determine whether the tobacco *TA29* gene 5' regulatory region could function in a distantly related plant and lead to male sterility. We obtained 24 *TA29-RNase T1* and 13 *TA29-barnase* transformants that contained one or two intact copies of the relevant *TA29-RNase* gene (data not shown). A male sterile phenotype that cosegregated with the *TA29-RNase* gene was observed in 71% (17/24) and 77% (10/13) of the *TA29-RNase T1* and *TA29-barnase* transformants, respectively. Compared with the flowers of untransformed oilseed rape plants (Fig. 3c), male sterile flowers (Fig. 3d) had slightly smaller petals, contained stamens that did not extend above the petals, and did not contain detectable pollen grains at anther dehiscence. In all other respects the male sterile oilseed rape plants were identical to untransformed controls, including the presence of well-developed nectaries (N) within their flowers (Fig. 3c, d).

We examined the anatomy of male sterile oilseed rape anthers present in 5-mm-long immature flower buds. Figure 4c shows a bright field photograph of a male fertile oilseed rape anther containing a well-formed tapetum (T) surrounding a pollen sac (PS) with developing pollen grains. By contrast, Fig. 4d shows that male sterile oilseed rape anthers containing a chimaeric *TA29-RNase* gene lack a detectable tapetum, and have irregularly shaped pollen sacs that do not contain visible microspores or pollen grains. Scanning electron micrographs of a rare pollen-like body present in only 2 of the 27 dehiscent male sterile anthers (Fig. 5d) showed that this structure was abnormal in size, and lacked a regular exine pattern compared with a normal oilseed rape pollen grain (Fig. 5c). Together, these data show that the tobacco *TA29* gene 5' region functions in oilseed rape anthers, that *TA29-RNase* gene expression selectively

destroys the tapetum, and that the absence of the tapetum leads to male sterile oilseed rape plants.

## Discussion

The experiments presented here show that the *TA29* gene 5' region programmes the expression of *GUS*, *RNase T1* and *barnase* genes specifically to anther tapetal cells, indicating that the *TA29* gene is regulated primarily at the transcriptional level. This finding is consistent with *TA29* gene run-off transcription studies (A. Koltunow and R.B.G., unpublished results), and with earlier population studies that showed that most anther-specific genes are under transcriptional control<sup>3</sup>. Recent studies have shown that only 0.3 kb of 5' sequence is required to programme both the temporal and cell-specific *TA29* gene transcription patterns during anther development (A. Koltunow and R.B.G., unpublished results). These studies suggest that transcriptional events occur during anther development to activate unique gene sets within the tapetum.

The phenotype of plants containing the chimaeric *TA29-RNase* gene strengthens our conclusion that the *TA29* gene is expressed exclusively in the tapetum in both tobacco and oilseed rape plants. If this gene were expressed at other times of the life cycle, the presence of RNase would have disrupted the normal course of vegetative and floral development. Destruction of the tapetum by *TA29-RNase* gene expression does not interfere detectably with anther development, suggesting that the tapetal cell lineage can be eliminated with no effect on subsequent stages of anther development. This result indicates that tapetal cells function autonomously, and that their continued presence is not required for the differentiation and/or function

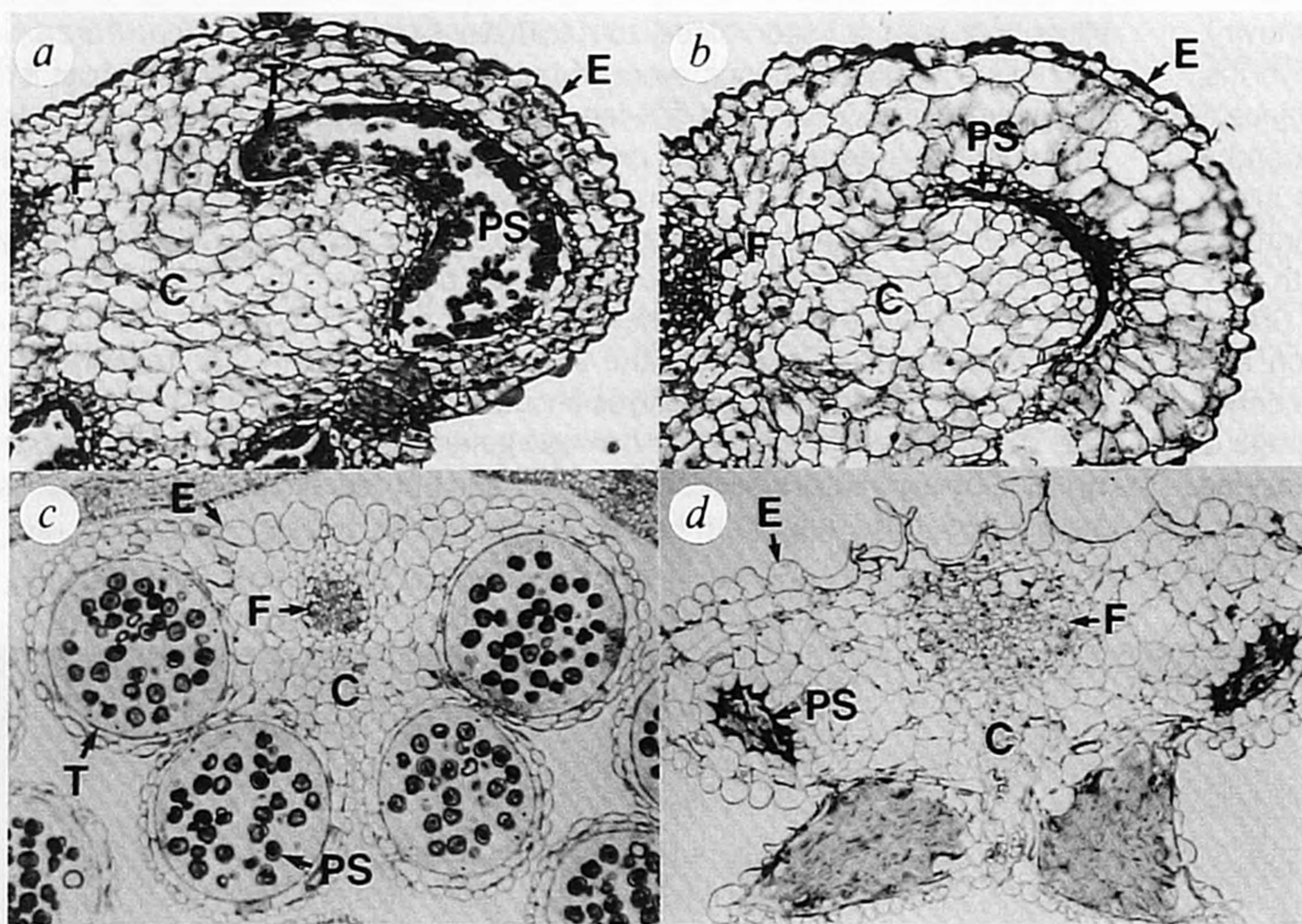
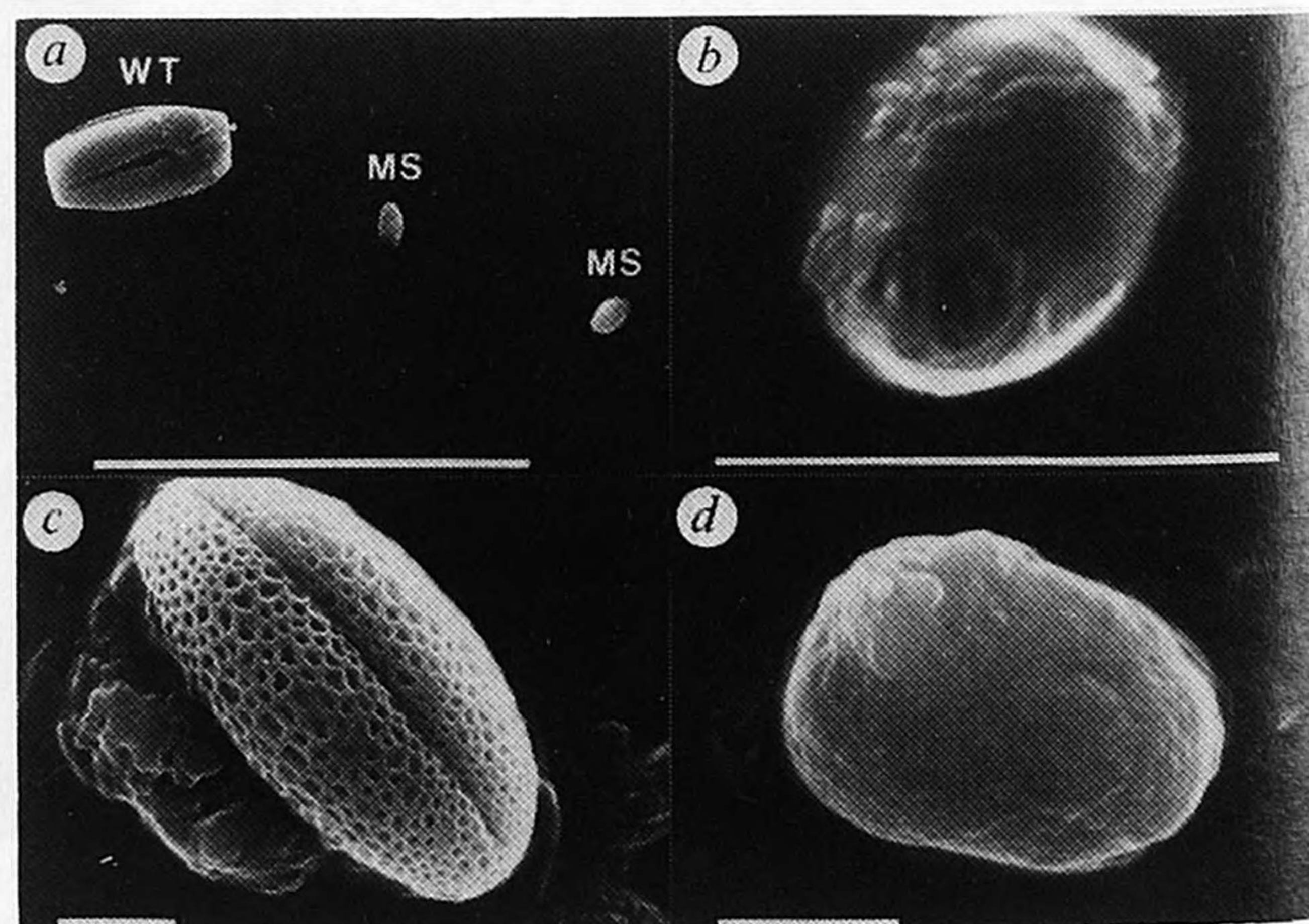


FIG. 4 Tissue abnormalities in male sterile tobacco and oilseed rape anthers. *a* and *b*, Bright field photographs of an untransformed tobacco anther (*a*), and a male sterile anther from a tobacco plant containing a *TA29-RNase* gene (*b*). C, E, F, PS and T, refer to connective, epidermis, filament, pollen sac and tapetum, respectively. *c* and *d*, Bright field photographs of an untransformed oilseed rape anther (*c*), and a male sterile oilseed rape anther from a plant containing a *TA29-RNase* gene (*d*).

METHODS. Stage 1 tobacco anthers were fixed and sectioned in a transverse orientation as outlined in the legend to Fig. 3. Oilseed rape anthers were harvested from 2.5-mm flower buds and fixed in glutaraldehyde<sup>21</sup>. Fixed anthers were embedded in LR-white, sliced into 1.5  $\mu$ m transverse sections with a glass knife, and stained with 0.05% toluidine blue.

FIG. 5 Scanning electron micrographs of pollen grains produced by male sterile tobacco and oilseed rape anthers. *a*, Tobacco pollen grains from untransformed anthers (WT), and anthers transformed with a *TA29-RNase* gene (MS). White bar, 100  $\mu$ m. Magnification,  $\times 710$ . *b*, Higher magnification of male sterile tobacco pollen grains shown in (*a*). White bar, 10  $\mu$ m. Magnification factor  $\times 9,150$ . *c* and *d*, Oilseed rape pollen grains from untransformed anthers (*c*) and anthers transformed with a *TA29-RNase* gene (*d*). White bars, 10  $\mu$ m. Magnification factors,  $\times 1,930$  and  $\times 2,980$  for the wild-type and male sterile pollen grains, respectively.

METHODS. Pollen grains were collected from dehiscenced anthers in open flowers (Fig. 4) and photographed in a scanning electron microscope<sup>28</sup>.



of anther cell types later in development.

The expression of either the *TA29-RNase T1* gene or the *TA29-barnase* gene leads to the production of male sterile plants. These plants are normal in all respects except failure to produce functional pollen. The tapetum is therefore essential for normal pollen development. Expression of both classes of RNase selectively destroyed tapetal cells, presumably by hydrolysing tapetal cell RNAs. An analogous process may occur naturally in the reproductive structures of self-incompatible plants<sup>17</sup>. Barnase seems to be more effective in tobacco than RNase T1. Genetic crosses with male sterile tobacco plants indicated that at least four *TA29-RNase T1* gene copies are required to produce male sterile anthers (C.M. and J.L., unpublished results). By contrast, only one *TA29-barnase* gene copy is required to produce male sterile plants in tobacco, and one copy of either the *TA29-RNase T1* or *TA29-barnase* gene is sufficient to produce male sterile oilseed rape plants. Because the same *TA29* gene 5' fragment was used in both chimaeric

*TA29-RNase* genes, these results suggest that RNase T1 is less active than barnase in tobacco tapetal cells.

The ability of the *TA29-RNase* gene to induce male sterility provides a new strategy for the production of hybrid crop plants. Transferring this dominant male sterility gene to plants such as corn should enable hybrids to be produced without mechanical removal of the anthers. By coupling the chimaeric *TA29-RNase* gene to a dominant herbicide gene (for example, *bar*; refs 18, 19), breeding systems can be devised to select for uniform populations of male sterile plants. In crop plants where fruit is not the harvested product (for example, lettuce, carrot, cabbage), male sterile plants can be crossed with any pollinator line to produce hybrid seeds. By contrast, in other crops such as tomato, wheat, rice and corn it will be necessary to restore full male fertility in the offspring. Antisense RNA technology<sup>20</sup>, and the existence of barstar, a protein inhibitor of barnase<sup>15,16</sup>, should facilitate the development of strategies for male fertility restoration. □

Received 11 July; accepted 24 August 1990.

1. Esau, K. *Anatomy of Seed Plants*. 2nd edn (Wiley, 1977).
2. Kamalay, J. C. & Goldberg, R. B. *Cell* **19**, 935-946 (1980).
3. Kamalay, J. C. & Goldberg, R. B. *Proc. natn. Acad. Sci. U.S.A.* **81**, 2801-2805 (1984).
4. Chapman, G. P. *Int. Rev. Cytol.* **107**, 111-125 (1987).
5. Mascarenhas, J. P. A. *Rev. Pl. Physiol. Pl. molec. Biol.* **41**, 317-338 (1990).
6. Knox, R. B. *Pollen and Allergy* (Arnold, London, 1979).
7. Kaul, M. L. H. *Monographs on Theor. and Appl. Genet. Vol. 10 Male Sterility in Higher Plants* (Springer, Berlin, 1988).
8. Goldberg, R. B. *Science* **240**, 1460-1467 (1988).
9. Seurinck, J., Truettner, J. & Goldberg, R. B. *Nucleic Acids Res.* **18**, 3403 (1990).
10. Varner, J. & Cassab, G. A. *Rev. Pl. Physiol. Pl. molec. Biol.* **39**, 321-353 (1988).
11. Condit, C. M. & Meagher, R. B. *Nature* **323**, 178-181 (1986).
12. Keller, B., Schmid, J. & Lamb, C. *EMBO J.* **8**, 1309-1314 (1988).
13. Jefferson, R. *Pl. molec. Biol. Rept* **5**, 387-405 (1987).
14. Quaas, R. *et al. Eur. J. biochem.* **173**, 617-622 (1988).
15. Hartley, R. W. *J. molec. Biol.* **202**, 913-915 (1988).
16. Hartley, R. W. *Trends biochem. Sci.* **14**, 450-454 (1989).
17. McClure, B. A. *et al. Nature* **342**, 955-957 (1989).

18. De Block, M. *et al. EMBO J.* **6**, 2513-2518 (1987).
19. Deblaere, R. *et al. Meth. Enzym.* **153**, 272-291 (1987).
20. Izant, J. G. & Weintraub, H. *Science* **229**, 345-352 (1985).
21. Cox, K. & Goldberg, R. in *Plant Molecular Biology: A Practical Approach* (ed. Shaw, C. H.) 1-35 (IRL, Oxford, 1988).
22. Jofuku, K. D. & Goldberg, R. B. in *Plant Molecular Biology: A Practical Approach* (ed. Shaw, C. H.) 37-66 (IRL, Oxford, 1988).
23. Maliga, P., Breznowitz, A. & Marton, A. *Nature* **244**, 29-30 (1973).
24. Horsch, R. *et al. Science* **223**, 496-498 (1984).
25. Perez-Grau, L. & Goldberg, R. B. *Pl. Cell* **1**, 1095-1109 (1989).
26. Cornelissen, M. & Vandewiele, M. *Nucleic Acids Res.* **17**, 19-29 (1989).
27. De Block, M., De Brouwer, D. & Tenning, P. *Pl. Physiol.* **91**, 695-701 (1989).
28. Fromme, H. G., Pfantsch, M., Pfefferkorn, G. & Bystziyky, V. *Microscopica Acta* **73**, 29-37 (1972).

ACKNOWLEDGEMENTS. We thank M. De Block, G. Engler, M. Habets and C. Tire for help with the anther sections; K. Cox for teaching us the *in situ* hybridization procedure; P. Stanssens and J. Steyaert for suggestions on RNases and for providing the *RNase T1* gene; R. Hartley for the *barnase* gene; M. Cornelissen and W. Timberlake for critically reading the manuscript; and V. Gossele, H. Van de Wiele, D. De Brouwer and C. Opsomer for technical assistance. Part of this research was supported by the National Science Foundation (R.B.G.).

## LETTERS TO NATURE

# A unified model of neutron-star magnetic fields

Roger W. Romani

Institute for Advanced Study, Princeton, New Jersey 08540, USA

**STRONGLY magnetized neutron stars are believed to be at the heart of a number of astrophysical systems, notably pulsars and X-ray binaries. Although the magnetic field is an important determinant in the behaviour of such systems, the origin and stability of the field is the subject of conflicting observational and theoretical evidence. Here I describe a new model of neutron-star magnetic moments, by which the fields are generated as the neutron star is born, and follow the evolution of the field over a Hubble time. With realistic thermal evolution and conductivities, isolated neutron stars will maintain large magnetic fields for more than  $10^{10}$  years. In addition, I show how mass accretion on to neutron stars can reduce the field strength<sup>1,2</sup>. This model of field generation and decay can explain a wide variety of observed systems.**

Newborn neutron stars are thought to have large dipole surface fields, as evidenced by spindown torques on young radio and X-ray pulsars. For a radio pulsar of period  $P$  spinning down in isolation, magnetic-dipole braking models give an estimate of the field at the surface

$$B_s \approx \left( \frac{3Ic^3 P \dot{P}}{8\pi^2 R^6} \right)^{1/2} \approx 1.0 \times 10^{12} (P \dot{P}_{-15})^{1/2} \text{ G} \quad (1)$$

where  $\dot{P}_{-15}$  is the pulsar period derivative in units of  $10^{-15} \text{ s s}^{-1}$ ,

$I$  the moment of inertia,  $R$  the radius and  $c$  the speed of light. For most known radio pulsars, the estimated surface field is  $\sim 10^{12.5} \text{ G}$ , with a dispersion<sup>3</sup> of  $\sim 10^{0.3} \text{ G}$ . The origin of this field is a subject of long-standing debate; a popular scenario involves flux freezing and amplification of interior fields of the progenitor object, which leaves the existence and magnitude of the characteristic value unexplained. Alternatively, it has been proposed that magnetic fields can be generated in young stars by thermomagnetic effects<sup>4</sup>.

The torque appears to decay on a timescale of several million years, leading to a rapid disappearance of the pulsars from the radio sky<sup>3,5</sup>. Recent observational and theoretical work has, however, clouded this picture appreciably. The binary and millisecond radio pulsars, in particular, make it clear that the fields of some neutron stars can be both a factor of  $\sim 10^4$  lower than the characteristic value and remain stable for  $\geq 10^9 \text{ yr}$  (ref. 6). Conversely, some  $\gamma$ -ray burst sources, believed to be old neutron stars, have been shown to have high surface fields of  $\geq 10^{12} \text{ G}$  (ref. 7); in addition, theoretical arguments<sup>8,9</sup> imply that it is difficult to reduce the magnetic flux threading much of the neutron-star interior.

Here I present a simple picture of the evolution of the magnetic field that explains the above behaviour. I assume that the field is generated after the birth of the neutron star during the initial cooling phase, either by thermomagnetic effects in the solid crust<sup>4</sup> or by dynamo processes in the still-liquid envelope above the solid interior. Thermomagnetic generation is most effective where the temperature gradient is steepest, that is, at the lowest solid densities. Similarly, dynamo-generated flux will be frozen into the star at the base of the liquid sea. Thus the yield stress